

DEVELOPMENT OF A PORTABLE SOLAR CONCENTRATION EQUIPMENT FOR WATER HEATING

BY

*CHIGBO EBENEZER .C (AGRICULTURAL AND BIORESOURCES ENGINEERING)

ORJI, CHUKWUDI. U (AGRICULTURAL AND BIORESOURCES ENGINEERING)

(MICHAEL OPKARA UNIVERSITY OF AGRICULTURE UMUDIKE, ABIA STATE, NIGERIA)

INEKWE GOZIECHUKWU (DEPARTMENT OF DIGITAL ENGINEERING, FACULTY OF

COMPUTER SCIENCE, OTTO VON GUERICKE UNIVERSITY, MAGDEBURG GERMANY)

ABSTRACT

In Nigeria, a country with an unstable power supply, the field of solar water heating technologies is expanding. This development of a portable solar water heating device was a pro-active reaction to the current energy shortage. The core of its thermal storage is made up of a buffer tank and a 5-liter insulated storage vessel. The assembly involves, a fine glazy reflector with a single glass sheet regulates the diverging rays. This was achieved by the use of a solenoid valve and a digital temperature sensor, two precise tools that helps to coordinate the flow of water inside the thermal storage reservoir. Notably, the arrangement has a serpentine-shaped flow channel thermal conductor pipe that skillfully promotes heat conduction.

The system was subjected to a six-day testing session. The greatest temperature recorded over the first three days of testing the solar water heater without a thermal collector was 51.3 °C, while a significant improvement in performance with a peak outlet temperature of 72 °C was observed with the integration of the thermal energy collector.

The efficiency peaked at 68.19% on the fourth day of testing. On the sixth day, the apex irradiance level reached $1074.0 \text{ W/}m^2$, with an outlet temperature of 72 °C. The fourth day had the greatest temperature increase, as evidenced by a rise of 47.1 °C between 10am and 12noon. Interestingly, day three recorded the lowest irradiance levels, showing the system's performance temporal swings. The system, distinguished by its optimal performance, yielded an efficiency of 98% at 3:15 pm on the fourth day, with a thermal energy dissipation between 4:15 pm and 5:45 pm during that day.

1. INTRODUCTION

In a prosperous society, energy is acknowledged as the main driver of economic and industrial progress. The prevention of poverty and assurance of human comfort depend on an adequate supply. Population and economic expansion, particularly in developing countries, are both contributing to a significant rise in energy demand worldwide. By 2035, it is anticipated that these markets would be responsible for 90% of the rise in energy consumption. The scarcity of energy has hampered economic progress in many developing countries, including Nigeria (Adedayo et al., 2021).

Nigeria, which has a surface area of 923,768 km2 and is situated between latitudes 4° and 14° North of the equator and longitudes 3° and 14° East of Greenwich, has a population of around 150 million. Nigeria is located in a region with abundant sunlight and great solar energy potential. Total solar radiation varies depending on location, from around 3.5 kWh/m2/day in coastal areas to about 7 kWh/m2/day in semi-arid regions in the country's far north. The nation receives around 6.8 hours of sunshine per day and 19.8 MJ/m2/day of solar energy on average. The distribution of solar radiation is generally good, with minimum averages in Katsina in January of around 3.55 kW/m2/day and 3.4 kWh/m2/day in Calabar in August, and highest averages in Nguru in May, among others (Ekechukwu et al., 2011). Nigeria's enormous solar resources offer a chance for the country to prosper by concentrating on the creation of solar-powered machinery and gadgets, such solar concentrator water heaters.

The fusion of hydrogen and helium atoms in the sun produces high-energy particles known as gamma rays, which have a magnitude of about 3.47221024 kW and are the source of solar energy. Electromagnetic energy is used to send these gamma rays to Earth. There are three types of this radiation: UV rays, visible light, and infrared rays. Through the use of photovoltaic (solar cell), solar collector, and solar concentrator technologies, the solar energy that reaches the Earth's surface may be directly captured. Electricity is produced using photovoltaics, while heat energy is produced using sun concentrators and collectors. The foundation of solar water heating technology is the conversion of radiation into heat energy using solar energy collectors (concentrators). Three components make up a simple solar water heater: a flow channel, a tank, and a collector.

Solar water heaters (SWH) have a long history that dates back to the Roman Empire approximately 200 B.C.E. The Romans created a straightforward method to heat their public baths using solar energy, eliminating the demand for coal and labor-intensive physical work. Although not entirely self-sufficient, these devices introduced the idea of solar water heating. After the fall of the Roman Empire, the practice of utilizing the sun

to heat water was completely forgotten. A Swiss natural scientist named De Saussure didn't revive the idea of utilizing solar energy for water heating until the late 18th century (1767). He built an insulated box, covered it with two panes of glass, and painted the bottom black to better absorb solar radiation. The basis for all succeeding solar water heaters was set by this prototype. De Saussure noticed that the insulated box heated up over the boiling point of water when exposed to sun light. In doing so, he provided the first proof of the greenhouse effect (Perlin, 2008). However, it took more than a century for scientists to realize the full potential of this ground-breaking gadget (Uwah, 2020).

Concerning the low level of knowledge about this technology among the tested population, a survey on solar water heating applications in households, schools, hospitals, and hotels undertaken by GIZ Nigeria in 2013 yielded frightening results. There are a few applications, mostly in Jos, Plateau State Nigeria, in some residences and schools, but there are also locally produced demonstration systems in research facilities in some parts of Nigeria like Nsukka and Sokoto. Official data on the contribution of solar thermal energy to overall energy consumption are not available, and these systems have not yet become widely used in Nigeria (Nwoke et al., 2015).

The distribution of energy demand is significant, according to statistical statistics. The total energy usage in Nigeria for the year 2012 was 116,457 ktoe (kilotons of oil equivalent). In light of this, it is clear that the residential sector distinguished itself as the largest energy consumer, as shown in Figure 1.

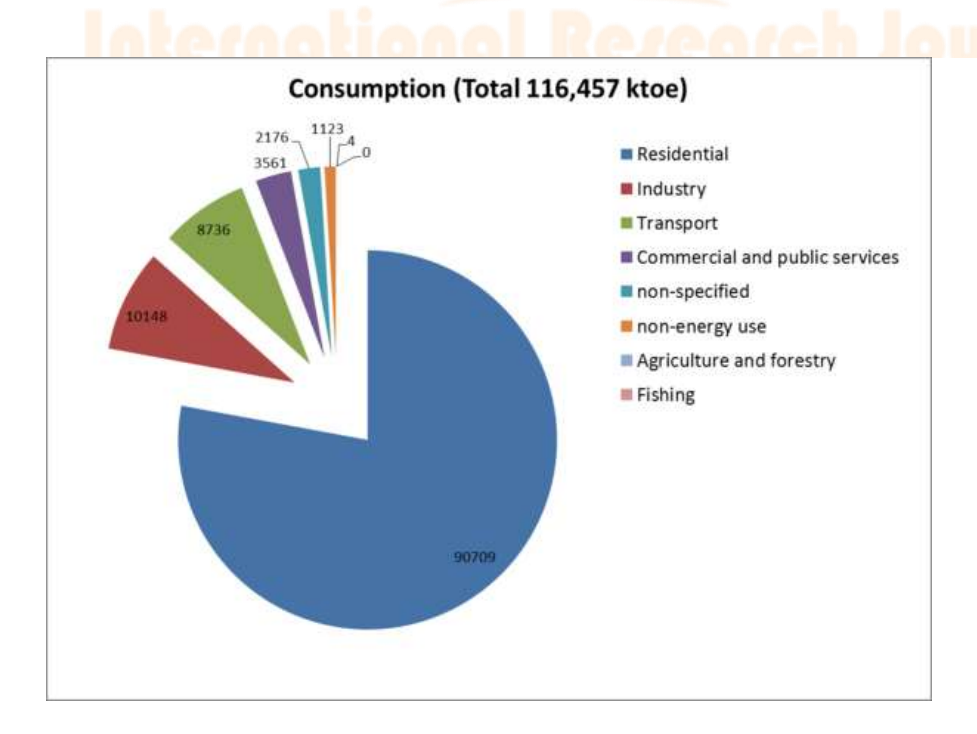


Fig 1. Total energy consumption by various sector in Nigeria in 2012 (energypedia, 2022)

However, a study shows that residential energy consumption is trending significantly upward. This large consumption is mostly caused by biofuels, which account for a significant 69.98% of the total energy produced. This method of energy production primarily entails cutting down trees. On the other hand, only 0.07% of energy is produced from renewable resources, which is disturbingly low. This group contains solar thermal energy and wind energy, both of which are easily available and suitable for human use (see Figure 2). Unfortunately, despite having a them in aboundance, these renewable resources are still largely underused.

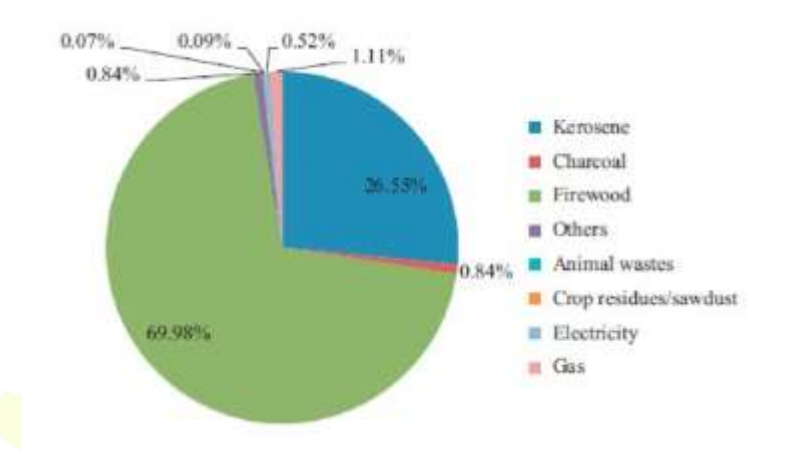


Fig 2. Consumption by source in Nigeria (Mohammed et al, 2013)

3. MATERIALS AND METHODS

The Solar Water Heater's dimensions and design makes it possible to choose materials that meet the requirements of the design. The flow channel, storage tank, and flat-plate collector are the main elements taken into account throughout the design phase.

Concentrating Solar Collectors

The solar concentrating collector is described by so many parameters as given below;

Aperture area A_q : This is the area of the collector that intercepts the solar radiation.

Acceptance angle: This is the angle through which a beam of light can be moved and still converge at the receiver. (Hsieh, 1986) A concentrator with small acceptance angle is required to track the sun continuously while. a concentrator with large acceptance angle needs only seasonal adjustment.

Absorber area Aabs: This is the total area of the absorber surface that receives the concentrated solar radiation. It is also the area from where useful energy can be extracted.

Concentration ratio C: This is defined as the ratio of the aperture area to the absorber area i

© 2025 IJNRD | Volume 10, Issue 1 January 2025 | ISSN: 2456-4184 | IJNRD.ORG $C = \frac{A_a}{A_{aba}}$ (1)

Optical efficiency: This is defined as the ratio of the energy absorbed by the absorber to the energy incident on the concentrator aperture (Garg and Prakash, 2000). It includes the effect of mirror/lens surface, shape and reflection/transmission losses, tracking accuracy, shading, receiver-cover transmittance, absorptance of the absorber and solar beam incidence effects. The optical efficiency is given as:

$$\eta_{o} = \frac{P_{abs}}{A_o I_D} \tag{2}$$

Where P_{abs} : This is the absorbed energy, A_o : This is the optical area

 \bar{I}_D : This is the incident light

The optical efficiency of most solar concentrators lies between 0.6 and 0.7.

Thermal efficiency is defined as the ratio of the useful energy delivered to the energy incident at the concentrator aperture:

$$\eta_{th} = \frac{Mc(T_{outlet} - T_{amb})}{I_b A_a} \tag{3}$$

Where M: This is the mass of the water

c: This is the specific heat capacity of water

 T_{outlet} : This is the outlet temperature

 T_{amb} : This is the ambient temperature

 I_b : This is the irradiance

 A_a : Thia is the area of the concentrator

 η_{th} : This is the thermal efficiency

The incident solar radiation consists of beam (direct) and diffuse radiation. However, the majority of concentrating collectors can utilize only beam radiation.

Instantaneous thermal efficiency of a solar concentrator may be calculated from an energy balance on the absorber. The useful thermal energy delivered by a concentrator is given by

$$q_u = \eta_o I_b A_a - U_L (T_{abs} - T_{amb}) A_{abs} \tag{4}$$

Where;

 q_u : This is the useful thermal energy

 T_{abs} : This is the temperature within the absorber

 U_L : This is the ultimate heat loss obtained by convection

Therefore, the instantaneous thermal efficiency may be written as

$$\eta = \frac{q_u}{I_b A_a} = \eta_o - \frac{U_L(T_{abs} - T_a)}{I_b C} \tag{5}$$

At higher operating temperatures the radiation loss term dominates the convection losses and the energy balance equation may be written as

$$q_u = \eta_o I_b A_a - U_L (T_{abs}^4 - T_a^4) A_{abs} \tag{6}$$

In Eq. (6) U_L takes into account the accompanying convection and conduction losses also. The instantaneous thermal efficiency η is now given by

$$\eta = \eta_o - \frac{U_L(T_{abs}^4 - T_a^4)}{I_b C} \tag{7}$$

Since the absorber surface temperature is difficult to determine, it is convenient to express the efficiency in terms of the inlet fluid temperature by means of heat removal factor F_R as:

$$\eta = F_R \left[\eta_o - \frac{(T_L - T_a)}{I_b C} \right] \tag{8}$$

The instantaneous thermal efficiency is dependent on two types of quantities, namely the concentrator design parameters and the parameters characterizing the operating conditions. The optical efficiency, heat loss coefficient and heat removal factor are the design dependent parameters while the solar flux, inlet fluid temperature and the ambient temperature define the operating conditions.

DESIGN CALCULATIONS

The heat demand load of the heater is such that it will heat about 5 litres of water in a day, from ambient temperature to 70 °C. Hence, in order to reduce space requirement, the heater was designed in such a way that it heats up about 10 centiliters of water only at a time. Thus, at an average uniform rate of solar insolation, the heater will make 6 cycles of almost equal lengths in time to heat the quantity of water required.

EXPECTED THERMODYNAMIC PERFORMANCE OF THE PTSWH

The estimated useful energy for one cycle of the designed PTSWH is given by

$$\tilde{\mathbf{e}}_u = \eta I_b A_a$$

Where \tilde{e}_u = estimated useful energy, I_b = solar irradiance, A_a = area of aperture

The efficiency range of most solar concentrators is 40% - 60% taking an average of 50% (B.S., 1993). Hence, Umudike solar radiation I_b is given as 5.89 MJ/ m^2 (1636.1W/ m^2) in January (Amadi, 2020):

$$\tilde{e}_u = \eta I_b A_a = 0.5 \times 1636.1 \times 721 = \frac{589814.05}{3600} = 163.83 \text{W/h}$$

For six cycles, the total useful energy is, $\tilde{E}_u = 6\tilde{e}_u = 6 \times 163.83$

$$\tilde{E}_u = 982.98 \text{ W/h}$$

The useful energy is also given by
$$\tilde{E}_u = \dot{m}_w c_{pw} (T_w - T_a) = \eta. \bar{I}_D. A_a$$
 (9)

Where \dot{m}_w = the rate of heating the water

 $c_{pw} = \text{specific heat capacity at constant pressure of the water.}$

 c_{pw} = properties of water was obtained as 4186J/kg K (at 25 °C) (Rogers et al, 1981)

$$\dot{\mathbf{m}}_w = \frac{\rho_w V_w}{t} \tag{10}$$

Where $\rho_w = \text{density of water evaluated at the temperature of } 25^{\circ}C$, and

$$t = \text{time taken to heat the water} = \frac{\rho_w V_w}{\dot{m}_w}$$
 (from eqn. 10)

For 6 cycles the total time, $t_t = 6 \times t$

The energy, Pabs, absorbed by the absorber was obtained from Eq. (2): $\eta_o = \frac{P_{abs}}{A_o \bar{l}_D}$

$$P_{abs} = \frac{\eta_o}{n} \left(\eta A_o \bar{\mathbf{I}}_D \right) \tag{11}$$

Determination of Hot Water Demand and Storage Tank Volume

The daily hot water demand was estimated for the design of the solar water heating system. Considering a domestic setting of a couple without any children where hot water is used for bathing, 15 litres of water was estimated to meet each individual's demands. The daily hot water demand was used to determine the storage tank volume as seen in Equation 12 (Technologies, 2011),

$$V_{st} = (l \times b \times h) \tag{12}$$

Where V_{st} = storage tank volume in litres, 10 litres

From this, V_{st} is calculated to be 10 litres.

Where b is the storage tank breath in m and l is the storage tank length, and h as the height of the tank.

Breath of tank = 20cm, Height of tank = 14.01cm, Length of the tank = 35.7cm

$$V_{st} = 10,000 \ cm^3$$

Determination of Thermal Energy Required

The amount of thermal energy required to heat up 1 litre of water is given by:

$$Q_{St} = \frac{\left(m C_W (T_{outlet} - T_{amb})\right)}{1000} \tag{13}$$

Where Q_{St} = amount of thermal energy in kWh required to heat up the total volume of water

 T_{amb} = ambient temperature

 T_{outlet} = outlet temperature

m = total mass in kg of the water to be heated and

Cw = specific heat capacity of water is 4.18 J/g °C.

Since mass is a function of volume and density, Equation 13 can be rewritten as:

$$Q_{St} = \frac{(\rho V_{St} C_w (T_o - T_i))}{1000}$$
 (14)

Where ρ = density of the water heated 997kg/ m^3 , T_{amb} is assumed to be 34°C and the desired temperature is 80°C. Hence from equation 14, $Q_{St} = 2.3$ kW/h

Determination of Design Month

From Table 2, January was chosen as the period for this experiment. Its average value gives an irradiance (I) of **5.89**MJm/m₂/day as the design value.

Table 2: Estimated global solar irradiance using meteorological parameters determined by the researchers source: (Amadi, 2020)

Month	Hm		Hp (M	(Jm-2)
s	(MJm-2)			
		S/Smax	RH	Tmax
1	5.89	5.99	6.15	5.89
2	5.41	6.94	6.51	6.24
3	6.95	5.29	6.04	5.59
4	6.03	5.23	5.76	5.25
5	6.2	4.67	4.5	4.48
6	3.42	4.56	3.67	3.17
7	3.03	3.65	3.77	3.19
8	2.23	3.81	3.66	3.29
9	2.8	4.11	3.86	5.22

10	© 20 4.76	25 IJNRD 4.68		10, Issue 1 January 2025 ISSN: 2456-4184 IJNRD.ORG 5.06
11	5.82	4.76	5.89	4.22
12	5.87	5.21	5.78	5.88

Collector Sizing Based on Heat Energy Required

The solar collector is sized according to the amount of heat energy required by the system. The irradiance values at the system site and the collector efficiency are also important in the determination of the collector area. Efficiency of the collector can be calculated by:

$$\eta = \frac{heat \ output}{heat \ input} = \frac{Q_{st}}{IA_c} \tag{15}$$

Where I is the solar irradiance in kWh/ m₂/day, η is the collector efficiency and A_c is the collector area in m₂. From Equation 15,

$$A_c = \frac{Q_{st}}{I\eta} \tag{16}$$

According to (Rikoto & Garba, 2015), collector efficiency is between 0.4 - 0.6, hence assuming an efficiency of 58% for the system design and with $I = 5.89 \text{ MWh/}m^2/\text{day}$, the collector area required to attain the thermal energy of 2.3 kWh was determined to be **0.76 m2**.

Determination of Flow Channel Diameter

The type of flow process was used to estimate the pipe's diameter. It is advised that the flow velocity of water in copper tubes not exceed 0.6 m/s when temperatures regularly surpass 60 °C. (ToolBox, 2005). This was taken into account when selecting a flow velocity, U, for the system design. The formula for calculating the heating time per flow cycle, tn, is as follows:

$$t = (t/n)1000 (20) (20)$$
 (17)

where t is the whole heating period (m), and 6 flow circles.

So tn = 3600 s/cycle.

The volumetric flow rate, V:
$$\dot{V} = \frac{VSt/1000}{tn}$$
 (18)Where $VSt = \text{storage}$

volume of 1 litre

tn = heating time per flow cycle in seconds/ cycle. This gave the volumetric flow rate as $1 \times 10^{-5} \ m^3/s$. For fluid flow, volumetric flow rate (\dot{V}) is expressed as:

$$\dot{\mathbf{V}} = A_f U \tag{19}$$

Where \dot{V} = volumetric flow rate (m^3/s) ,

 $Af = \text{flow area in } (m^2), U = \text{flow velocity of } 0.1 \text{ m/s}.$

Equation 19 can also be expressed in terms of the pipe diameter as:

$$dp = \sqrt{4}\dot{v}/\pi U \tag{20}$$

Where dp = pipe diameter in metres,

from Equation 20, the pipe diameter was determined

Determination of Storage Tank Insulation Thickness

For heat transfer across a wall, the heat loss is given by the fourier rate equations Q = -kA (dt/dx) may be separated and integrated directly between the limits $t = t_1$ at x = 0 and $t = t_2$ at $x = \delta$

$$Q = \frac{t_{o-t_i}}{\frac{\delta}{kA}} = \frac{t_{o-t_i}}{R_t} \tag{21}$$

Where R_t =thermal resistance to heat flow

K= thermal conductivity of polystyrene

A= area of thermal tank

 δ = wall thickness of thermal tank

 t_i = fluid temperature (°C),

 t_0 = temperature outside the tank (°C),

The insulation material is polystyrene, The thermal conductivity of solid nonporous polystyrene is taken to be 0.150 W/m·K and density 1050 kg/m³ at 9.85°C (Algaer, 2010)

Determination of parabolic trough

The parabola trough was determined by using length of chord of the circle which the parabola is part of as 10cm.

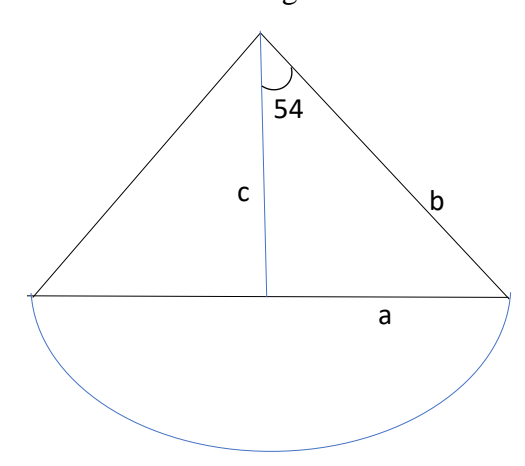
The radius was determined by dividing the chord from the centre of the diameter, then applied the following

euation;

$$\frac{\sin A}{a} = \frac{\sin B}{b} = \frac{\sin C}{c}$$

$$\frac{\sin 54}{5} = \frac{\sin 90}{b}$$

Where A, B,C,a,b and c are as shown in the diagram below.



b = 6.18cm

Determination of parabolic trough focal point

The diameter of the highest part of the parabola rim is measured as 100mm. Using the focal length parabola

formula
$$f = \frac{r^2}{4h}$$

Where r = radius of the diameter

h = vertical depth of parab



Figure B10: Fabricated solar water heater with thermal energy collector

4. RESULT AND DISCUSSION

The data required for the performance analysis of the PTSWH is shown in table 4.1. The experiments were conducted within three days. The first three days were computed without attaching a thermal collector and a glazing material.

 T_1 = Temperature of pipe on trough 1(inlet temperature)

 T_3 = Temperature of pipe on trough 3

 T_5 = Temperature of pipe on trough 5

 T_6 = Temperature of pipe on trough 6

 T_{outlet} = Temperature of water at the outlet point.

Table 4.1 Reading for the first day of experiment (12/01/2023)

Time	Ambient	T_1	T_3	T_5	T_6	T _{outlet}	Irradiance	Thermal
(h)	temp	(°C)	(°C)	(°C)	(°C)	(°C)	W/m^2	Efficiency
	(°C)	9						(%)
10:15	30.2	31.0	31.2	32.7	32.1	35.7	665.1	23.29
10:45	32.6	34.7	33.1	34.5	34.2	37.6	733.5	19.21
11:15	33.9	35.0	33.9	38.2	36.4	42.4	787.6	31.48
11:45	34.2	35.8	34.4	40.1	38.0	44.3	836.5	34.02
12:15	34.6	36.5	36.9	44.6	40.9	48.2	838.2	45.71
12:45	35.2	38.6	39.4	44.6	41.3	48.0	799.7	45.11
1:15	38.6	40.1	36.4	43.2	41.8	47.6	783.4	32.36
1:45	38.2	39.1	38.6	43.7	43.4	47.4	731.6	35.43
2:15	36.2	36.6	37.1	44.5	42.8	45.8	657.7	41.12
2:45	38.1	39.0	35.1	42.8	40.9	43.9	563.6	29.00
3:15	38.4	40.9	34.9	43.0	41.4	43.4	484.3	29.10
3:45	34.6	35.0	34.5	40.5	39.2	42.2	361.8	59.20
4:15	34.0	35.6	34.3	39.8	38.5	40.5	262.4	69.80
4:45	33.8	34.7	34.3	35.8	35.7	36.9	183.4	47.63
5:15	30.1	32.4	32.5	34.5	34.2	35.2	120.3	119.45

				0 = 0 =		. 0101110 1	o, 100 ao 1 jama	ar j = 0 = 0 1001	
5:45	29.8	30.3	30.2	31.9	32.0	32.8	55.7	151.76	

Table 4.1 shows that between 5:15pm and 5:45pm the efficiency was above 100%. This means the thermal energy was stored in the thermal collector.

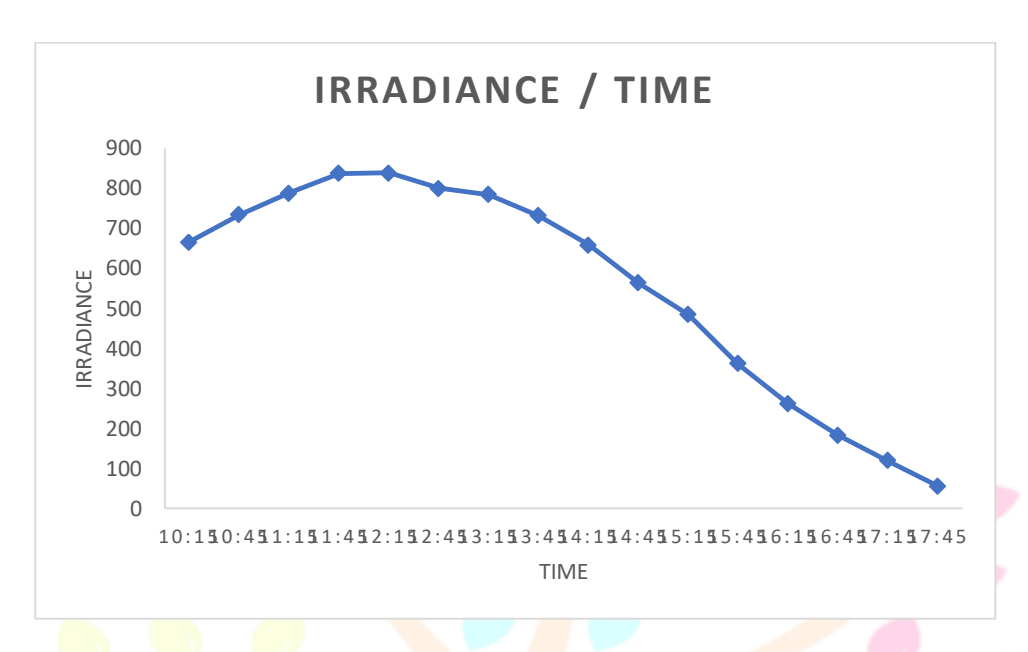


Fig. 11: Day 1 irradiance (10:15am – 5:45pm)

From this chart it was observed that the pick irradiance for day one was between 11: 45am and 12:15pm.

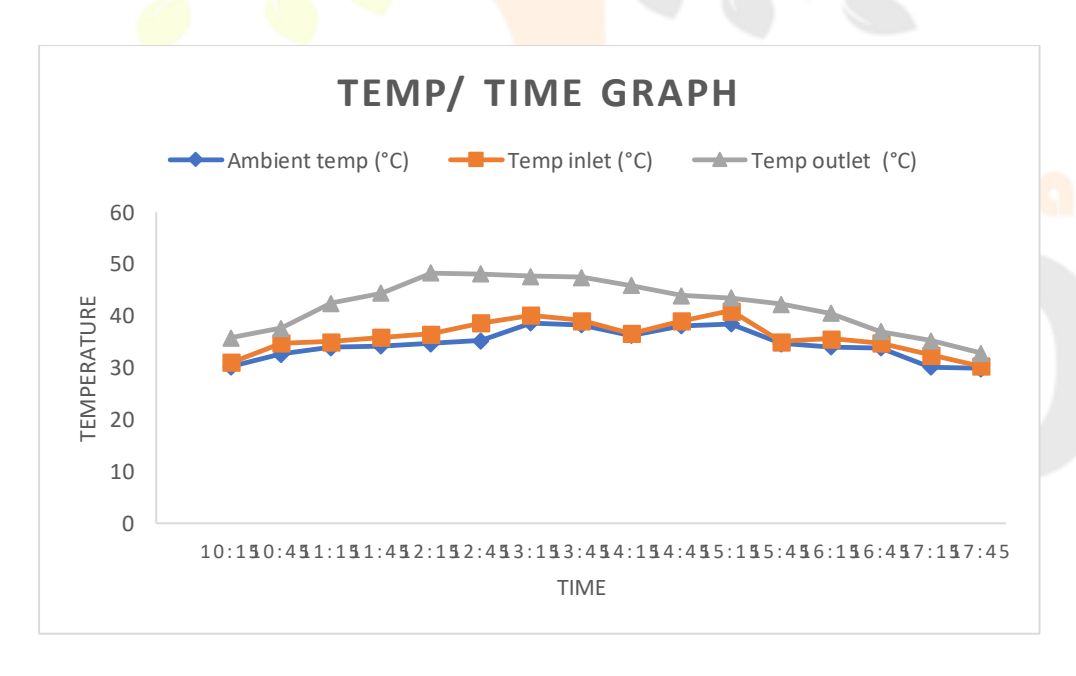


Fig. 12: Day 1 temperature gradience (10:15am – 5:45pm)

The output temperature at day one is shown to have its peak temperature by 12:15pm with a temperature of 48.2°C, while the inlet at 15:15 has its peak with a temperature of 40.9 °C and the ambient has at 13:15 with the temperature of 38.6 °C.

Table 4.2 Reading for the second day of experiment (13/01/2023)

Time	Ambient	T_1	T_3	T_5	T_6	T_{oulet}	Irradiance	Efficiency
(h)	temp (°C)	(°C)	(°C)	(°C)	(°C)	(°C)	W/m^2	(%)
10:15	32.7	33.2	32.8	33.9	34.1	35.9	816.4	11.04
10:45	34.6	35.2	34.8	35.1	35.5	36.6	830.5	6.80
11:15	35.8	36.4	37.4	36.2	35.4	37.4	878.2	5.13
11:45	36.0	36.8	40.2	37.3	36.9	46.2	875.2	32.84
12:15	36.7	37.5	42.1	40.1	38.8	47.4	886.1	34.02
12:45	36.4	37.4	41.7	42.6	40.8	49.8	854.9	44.16
1:15	38.3	39.6	41.9	42.3	41.0	49.9	823.4	39.70
1:45	39.1	40.4	41.1	41.5	40.7	49.5	776.8	37.72
2:15	39.6	41.3	41.4	42.3	41.4	51.3	743.8	44.32
2:45	39.4	42.8	43.5	43.8	42.5	48.7	667.6	39.25
3:15	40.1	41.1	40.7	41.1	40.5	45.5	542.8	28.03
3:45	39.2	41.0	40.6	45.4	42.9	44.3	446.6	32.18
4:15	37.5	38.8	39.2	41.0	39.6	42.0	351.4	36.08
4:45	35.6	36.9	37.5	39.5	38.7	40.0	228.6	54.23
5:15	32.8	34.4	35.8	36.6	35.7	39.2	116.8	154.39
5:45	28.7	31.6	33.4	33.4	33.1	37.9	54.9	472.16

Table 4.2 shows the efficiency exceeded 100% between 5:15pm and 5:45pm, which means there was thermal energy stored at that time, which resulted to a change in the trend of the temperature over each cycle.

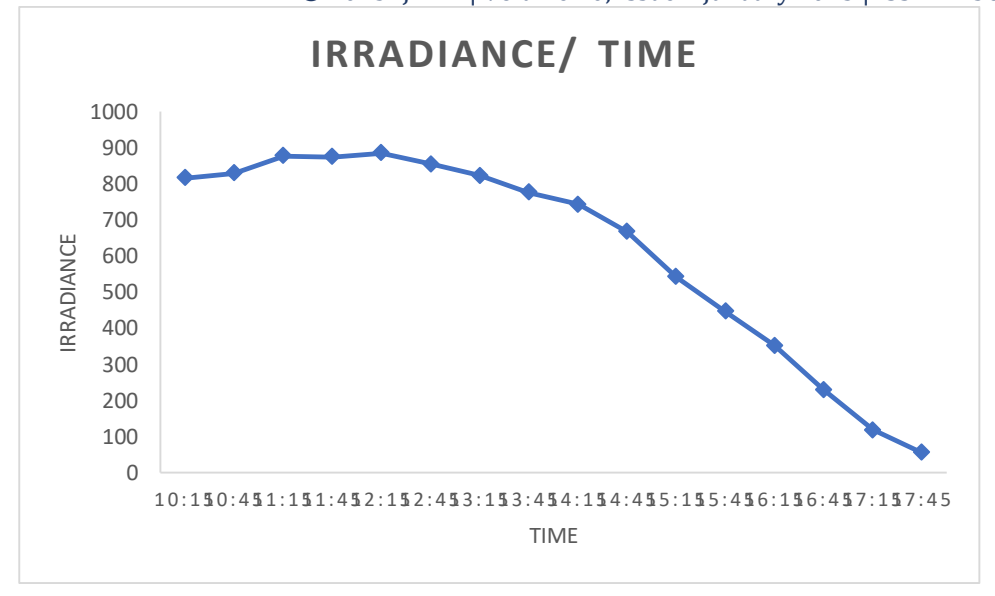


Fig. 13: Day 2 irradiance (10:15am – 17:45pm)

Fig. 13 shows that the solar radiation on day 2 was at its peak by 12:15pm with an irradiance of 886.1 W/m^2

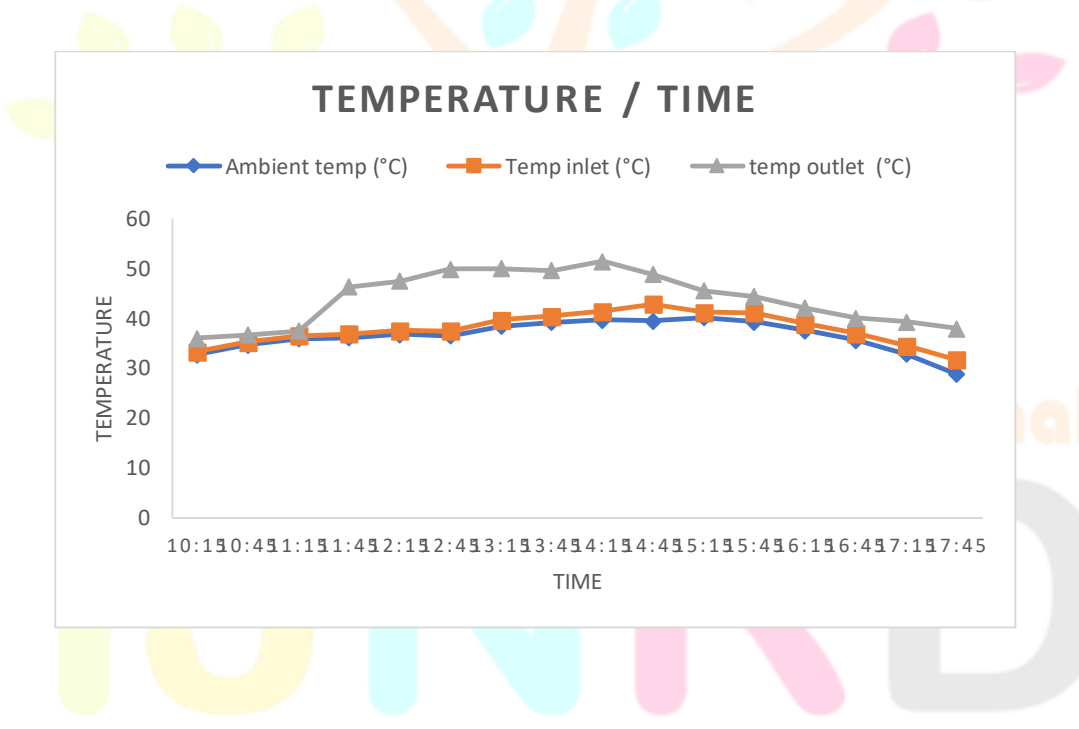


Fig. 14: Day 2 temperature gradience (10:15am – 17:45pm)

Fig. 14 reveals that the ambient temperature ranged between 28.7 - 40.1°C having its peak temperature by 3:15pm, the inlet temperature is slightly above the ambient temperature having its peak temperature at 42.8°C which shows the presence of heat and mass transfer from the surrounding to the systems inlet. The peak outlet temperature is shown to be at 51.3 °C by 2:15pm.

Table 4.3 Reading for the third day of experiment (16/01/2023)

Time	Ambient	<i>T</i> ₁	T_3	T_5	T_6	Toutlet	Irradiance	Efficiency
(h)	temp (°C)	(°C)	(°C)	(°C)	(°C)	(°C)	W/m^2	(%)
10:15	29.8	30.7	33.4	32.1	31.3	32.9	719.6	12.14
10:45	34.0	35.0	36.3	34.9	35.1	34.9	716.5	3.54
11:15	36.1	37.4	34.8	37.6	34.7	36.8	875.4	2.25
11:45	36.3	37.7	38.2	39.0	35.7	37.8	708.4	5.97
12:15	37.8	41.5	37.0	40.0	37.5	39.1	937.7	3.91
12:45	38.1	42.6	41.7	45.6	40.5	40.6	834.5	8.44
1:15	39.7	44.4	43.1	48.7	42.7	42.6	867.3	9.42
1:45	40.6	45.2	43.1	50.4	46.1	43.9	816.6	11.39
2:15	41.4	46.0	44.5	49.6	44.3	44.9	779.1	12.66
2:45	41.5	43.4	43.5	47.3	43.7	42.3	655.2	3.44
3:15	41.9	42.5	41.7	48.5	43.6	42.3	512.5	2.20
3:45	39.8	40.0	39.8	45.5	39.7	40.9	445.2	7.00
4:15	35.1	36.5	36.9	38.2	36.6	37.8	189.8	40.10
4:45	33.9	34.2	34.3	34.6	34.4	35.1	101.3	33.38
5:15	33.7	34.2	34.6	36.5	35.4	35.2	148.4	28.48
5:45	33.6	35.0	35.8	36.6	35.5	35.9	124.4	52.09

Table 4.3 shows the peak ambient temperature to be 45.4 °C which was obtained by 2:15pm and has the lowest at 29.8 °C by 10:15am because the sun was just rising. The peak out let temperature was recorded at 44.9 °C by 2:15pm which indicates the temperature was obtained between 12:15pm and 2:15pm, while the lowest outlet temperature was recorded at 32.9 °C.

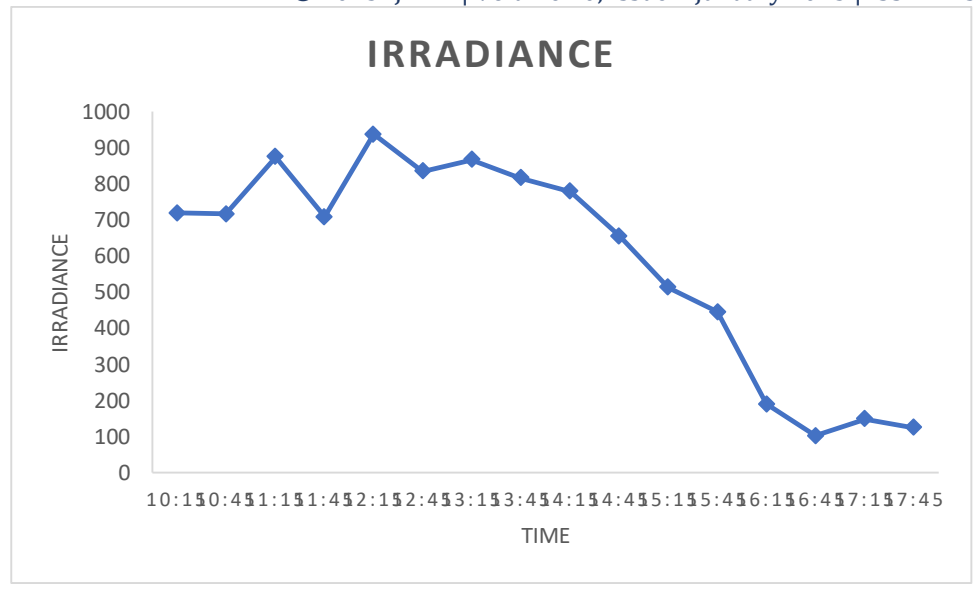


Fig. 15: Day 3 irradiance (10:15am – 17:45pm)

The peak of the solar radiation for the 3^{rd} day was recorded aS 937.7 W/ m^2 at noon (12:15pm) and the lowest irradiance was recorded at 52.09 W/ m^2 . The chart is not a steady flow chart because of the interruption of the irradiance by cloud.

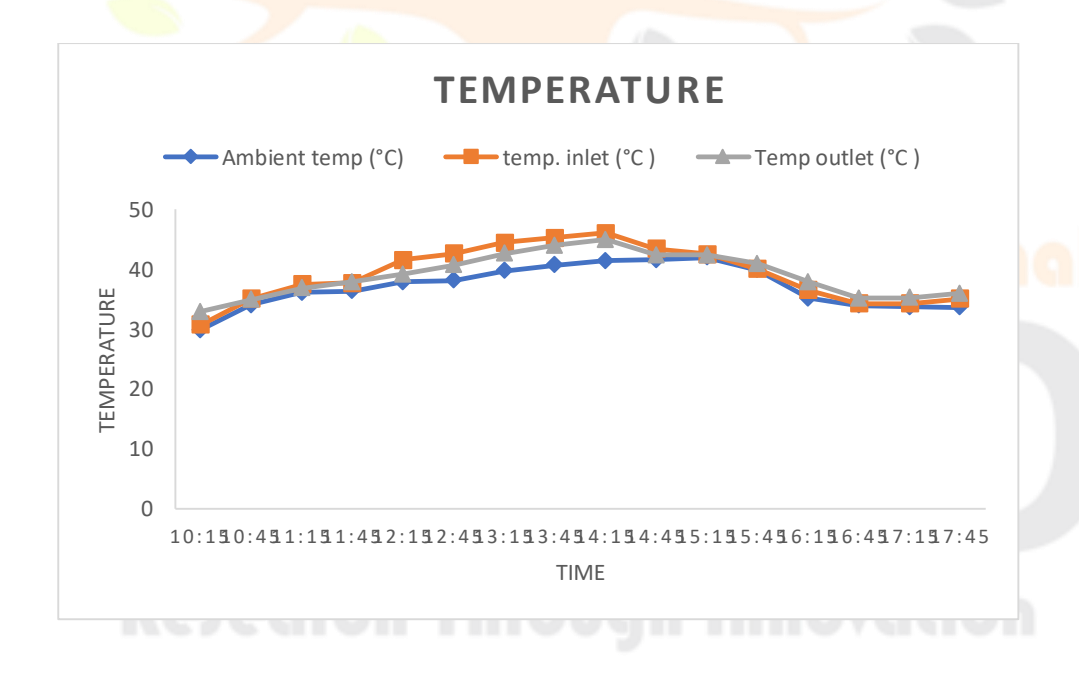


Fig. 16: Day 3 temperature gradience (10:15am – 17:45pm)

Fig. 16 shows that day 3 has its peak ambient temperature of 45.4 (°C) at 14:15pm and the inlet temperature of 46 °C by 14:15pm and the outlet temperature of 44.9 °C which indicates a flow in heat and mass transfer of the system. The chart is a continuous flow chart but with a change at the ambient temperature which distorted the flow between 3:15pm and 3:45pm with a temperature of 41.9 and 39.8 °C respectively.

The experiment carried out on the first three days experienced cooling from wind which could have resulted to the low efficiency recorded within those days.

Experiment taken with the presence of thermal energy collector

This second phase of experiment was carried out with a glazing material and a thermal collector designed with ply board to determine the thermal efficiency of the parabolic trough solar water heater using concentrators. This experiment was designed to last for three days.

Table 4.4 Reading for the 4th day of experiment (25/01/2023)

Time	Ambient	T _{inlet}	<i>T</i> ₃	T ₅	T ₆	Toutlet	Irradiance	Efficiency
(h)	temp (°C)	(°C)	(°C)	(°C)	(°C)	(°C)	W/m ²	(%)
10:15	35.8	36.7	47.5	47.4	48.0	47.9	658.3	51.8
10:45	37.1	38.6	48.9	48.5	49.7	49.5	712.4	49.0
11:15	36.0	50.4	59.5	57.8	54.4	54.1	539.4	94.5
11:45	35.2	51.4	64.5	65.7	60.4	60.0	955.7	73.1
12:15	38.1	45.0	70.3	66.3	59.3	59.1	947.2	62.5
12:45	36.2	54.8	73.2	70.2	72.2	72.0	1034.0	97.6
1:15	40.4	59.1	74.6	74.2	65.4	64.9	985.4	70.1
1:45	44.5	61.7	70.7	61.8	64.8	64.6	946.5	59.8
2:15	38.9	58.9	76.9	70.9	65.3	65.2	901.9	82.2
2:45	40.0	46.7	75.1	76.9	63.1	63.1	819.6	79.1
3:15	35.5	42.6	68.0	71.1	59.8	59.6	693.1	98.0
3:45	48.1	56.6	59.8	60.4	58.3	58.3	571.4	50.3
4:15	37.5	52.3	53.4	54.8	57.0	56.8	428.6	126.9
4:45	38.6	39.6	58.2	51.0	57.7	57.4	294.4	180.0
5:15	34.1	44.3	51.2	50.5	46.5	46.3	186.2	184.6
5:45	31.8	34.9	44.3	43.0	41.3	41.2	82.6	142.2

Table 4.4 shows that the efficiency exceeded 100% from 4:15pm to 5:45pm. This shows that with the presence of the glazing material heat is stored over a longer period of time

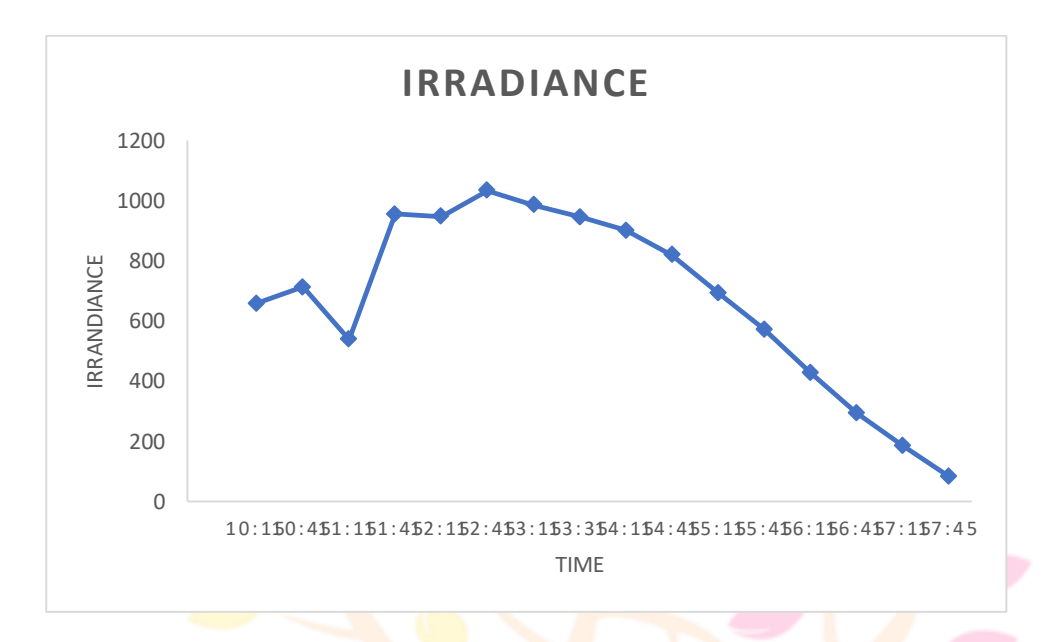


Fig 17: Day 4 irradiance (10:15am-17:45pm)

Fig 17 shows that the chart is not a steady chart with the change noticed at 539.4 W/ m^2 by 11:15am which could have been caused by weather change (cloud) during the sunshine hours which can alter the radiation flow. The lowest irradiance of the sunshine hours recorded was 82.6W/ m^2 .

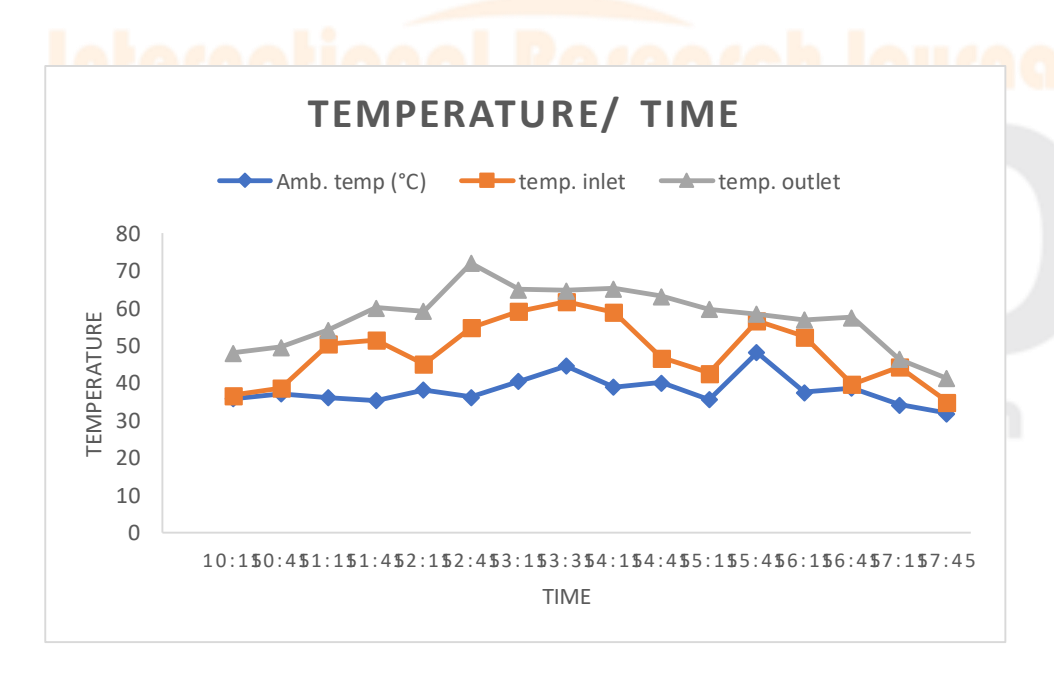


Fig 18: Day 4 temperature change (10:15am – 17:45pm)

Fig 18 shows that the temperature at day 4 has its peak ambient temperature of 44.5 °C corresponding with the irradiance of 946.5W/ m^2 all recorded at 1:45pm. Comparing the temperatures recorded shows a steady flow in the graph.

Table 4.5 Reading for the 5th day of experiment (26/01/2023)

Time	Ambient	T _{inlet}	T_3	T_5	T_6	Toutlet	Irradiance	Efficiency
(h)	temp (°C)	(°C)	(°C)	(°C)	(°C)	(°C)	W/m^2	(%)
10:15	31.5	33.0	47.3	47.8	47.4	48.6	654.1	73.6
10:45	37.2	35.2	59.9	60.7	58.2	49.1	791.4	42.4
11:15	32.0	35.4	56.1	55.1	52.0	46.4	156.5	259.4
11:45	33.9	48.9	51.4	52.3	49.6	42.8	999.7	25.1
12:15	33.3	59.7	66.4	61.9	55.7	49.0	219.8	201.3
12:45	38.2	52.5	52.5	58.8	50.2	43.7	247.2	55.9
1:15	36.1	69.6	73.6	70.3	59.7	52.4	568.4	80.8
1:45	39.1	51.1	82.5	79.9	65.7	59.3	885.6	64.3
2:15	38.1	49.4	72.6	73.1	61.9	57.8	769.6	72.1
2:45	39.7	59.1	78.0	77.1	66.5	60.9	761.7	78.4
3:15	42.1	49.5	76.6	75.7	60.3	63.2	667.3	89.1
3:45	37.3	51.4	71.2	70.5	65.6	61.7	559.4	122.9
4:15	37.0	46.3	53.8	50.1	51.7	51.3	390.9	103.0
4:45	39.5	45.6	52.7	44.8	46.1	45.3	271.1	60.3
5:15	33.2	34.7	45.6	41.3	42.1	42.6	139.1	190.4
5:45	31.7	36.6	38.4	34.8	32.6	36.8	53.1	270.7

Table 4.5 shows the efficiency to have a lot of irregularities caused by a lot of unsteady flow obtained at the irradiance as shown in fig. 19. An efficiency of 201.3% was recorded at 12:15pm corresponding with the 219.8 W/m^2 irradiance drop at same time. This indicates presence of clouds which prevent proper radiation to the earth surface.

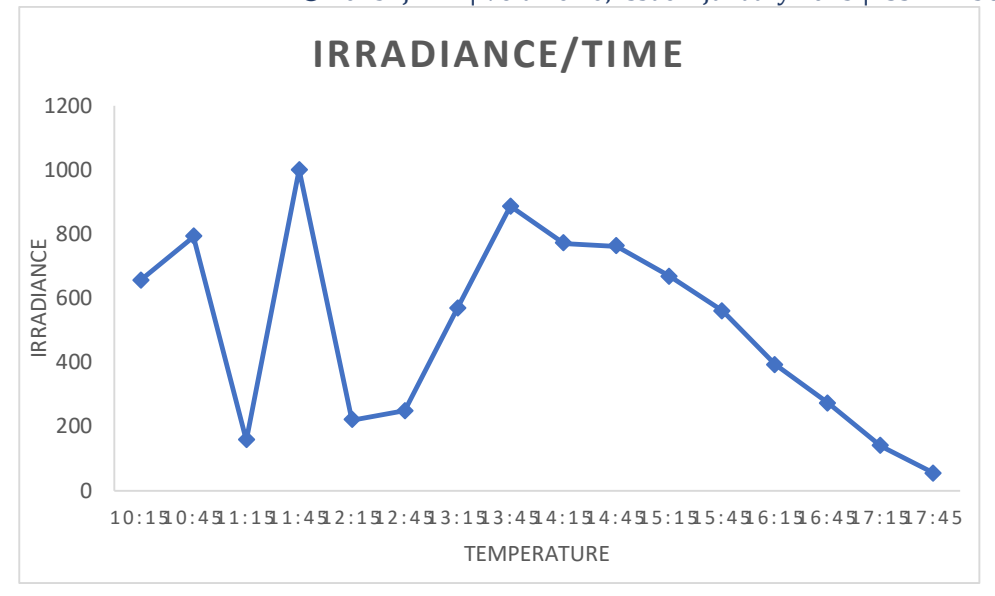


Fig 19: day 5 irradiance (10:15am – 17:45pm)

The day 5 irradiance shows that there was unstable intensity of the solar radiation between 10:15am and 13:45pm and became steady till 17:45pm. It is also noticed that the peak irradiance was 999.7 W/ by 11:45am and lowest irradiance $53.1 \text{ W/}m^2$ by 17:45pm.

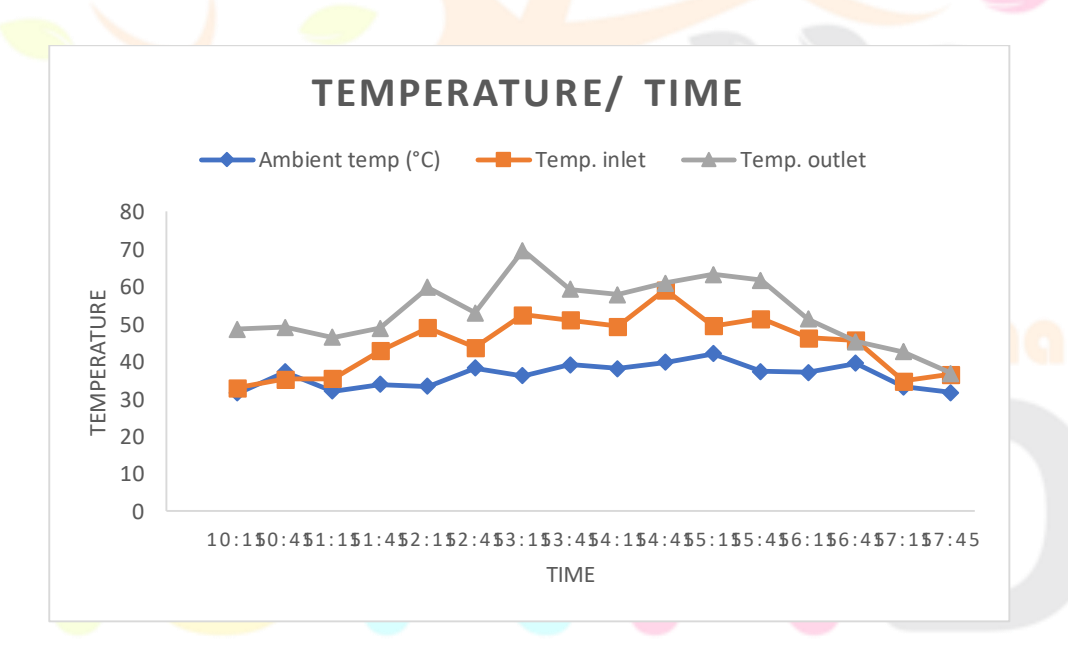


Fig. 20: the day 5 temperature change from 10:15 – 17:45

The day 5 temperature chart shows that the highest recorded temperature at the outlet was 69.6 °C by 13:15 (1:15PM), the ambient temperature 42.1 °C at 15:15 (3:15 PM) and the inlet temperature at 59.1 °C at 14:45 (2:45 PM).

Table 4.6 Reading for the 6th day of experiment (27/01/2023)

Time	Ambient	T_{inlet}	T_3	T_5	T_6	Toutlet	Irradiance	Efficiency
(h)	temp (°C)	(°C)	(°C)	(°C)	(°C)	(°C)	W/m^2	(%)
10:15	32.6	54.4	50.6	51.5	54.6	54.5	840.7	73.4
10:45	34.5	55.1	56.3	58.6	60.2	59.8	676.4	105.4
11:15	30.0	46.7	49.8	54.1	57.9	57.2	874.0	87.7
11:45	34.9	48.5	48.9	53.6	56.7	56.3	938.7	64.2
12:15	33.4	56.4	56.9	57.2	59.3	58.6	836.5	84.9
12:45	37.2	52.6	54.7	56.0	58.4	57.8	997.8	58.2
1:15	37.1	52.0	53.6	55.8	56.6	56.0	896.0	59.4
1:45	40.6	67.4	67.8	69.2	70.1	68.9	998.5	53.3
2:15	39.9	64.9	66.4	68.3	68.9	68.2	782.0	102.0
2:45	41.1	68.2	69.4	70.4	69.5	68.7	895.2	86.9
3:15	40.7	52.7	56.1	69.5	70.5	69.4	879.2	92.0
3:45	40.2	49.9	51.2	60.7	62.7	61.3	798.3	74.5
4:15	37.4	46.1	47.5	52.5	53.8	53.2	561.9	79.2
4:45	37.5	40.2	40.9	46.1	50.2	49.7	381.7	90.1
5:15	36.6	39.6	40.2	42.8	46.4	45.9	121.0	217.0
5:45	32.8	35.3	37.2	39.4	41.0	39.77	82.2	237.0

Research Through Innovation

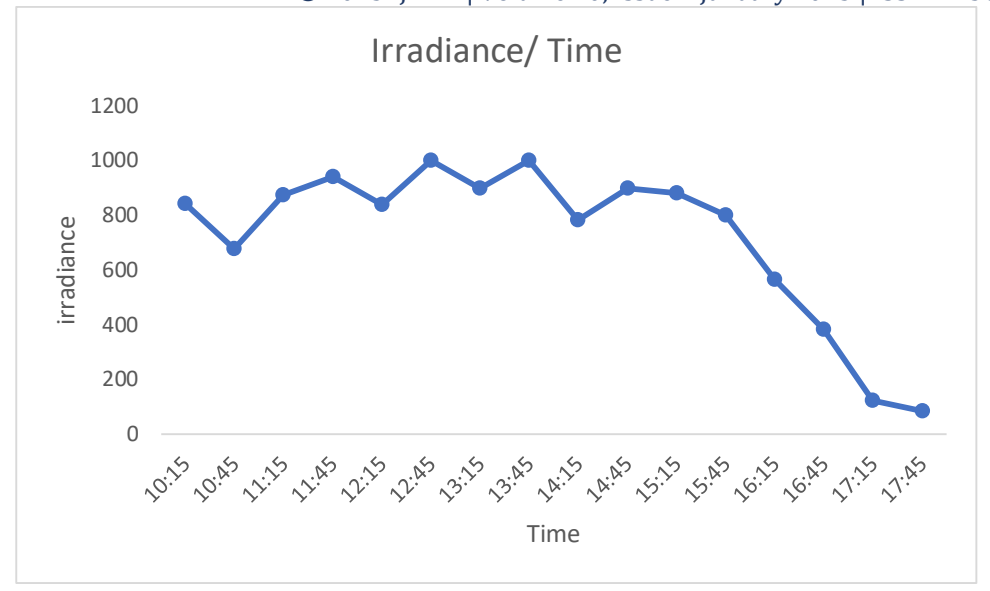


Fig.21: Day 6 irradiance (10:15am – 17:45pm)

The irradiance was highest by 13:45 and next to it was by 12:45. These shows that the peak of the solar radiation is between 12:45 – 13:45 ranging from 997.8 - 998.5 W/m2. Day 6 had the longest cloud interruption of the solar radiation ranging 10:15am to 14:15pm.

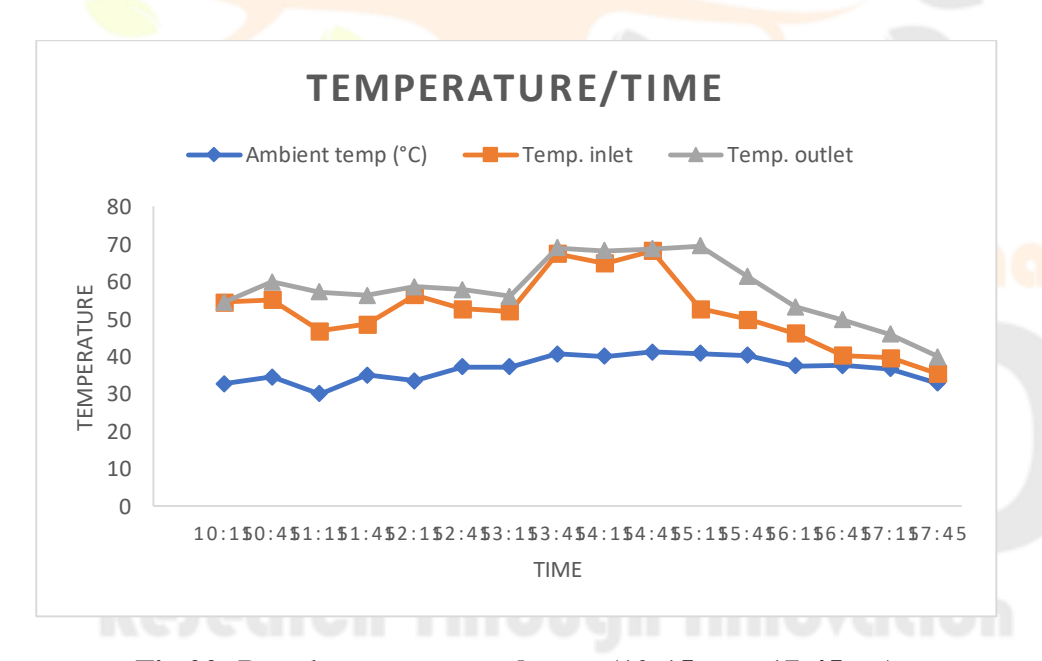


Fig 22: Day 6 temperature change (10:15am – 17:45pm)

From this fig. 22, it was observed that the highest temperatures of the day was at 13:45pm at 68.9 °C and 15:15pm at 69.4 °C while at the ambient it was 14:45 at 41.1 °C which indicates the stability of the irradiance as shown in fig. 21. The temperature of the inlet and outlet between 13:45pm and 15:15pm was observe to have a higher

variance from the ambient temperature which could be traced back to fig. 21 which shows that the highest range of irradiance ranging was from 782.0, 895.2 and $998.5 \text{W/}m^2$.

Comparing Average results from the first three days and second three days

Table 4.7: Comparing the temperature, irradiance and efficiency for the heater without glazing surface.

Days	Ambient	Outlet	Irradiance	Efficiency
	Temperature	temperature	(W/m^2)	(%)
	(°C)	(°C)		
1	34.5	37.5	166.6	50.9
2	36.4	39.3	184.1	40.2
3	37.1	38.4	176.2	14.8

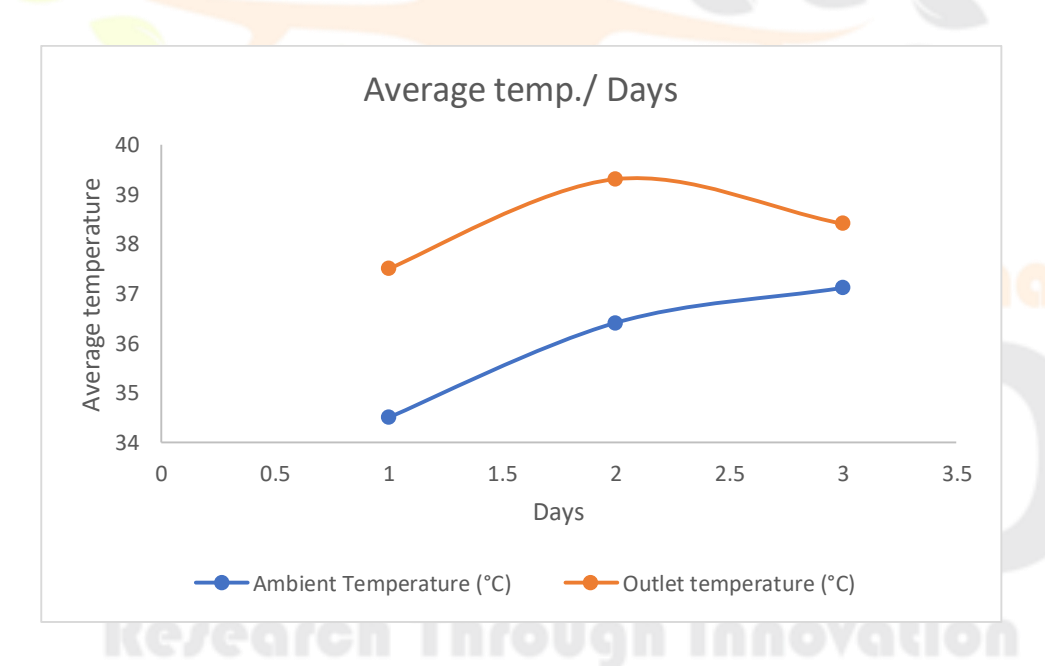


Fig. 23: comparing the average temperature of days readings without heat collectors

Fig. 23 provides a graphical data for the averages of both ambient temperature and outlet temperatures respectively. It shows a corresponding flow between the outlet temperature and irradiance (fig. 24.), while the ambient temperature had its peak temperature on the third day (37.1 °C) and lowest temperature on the first day(34.5 °C).

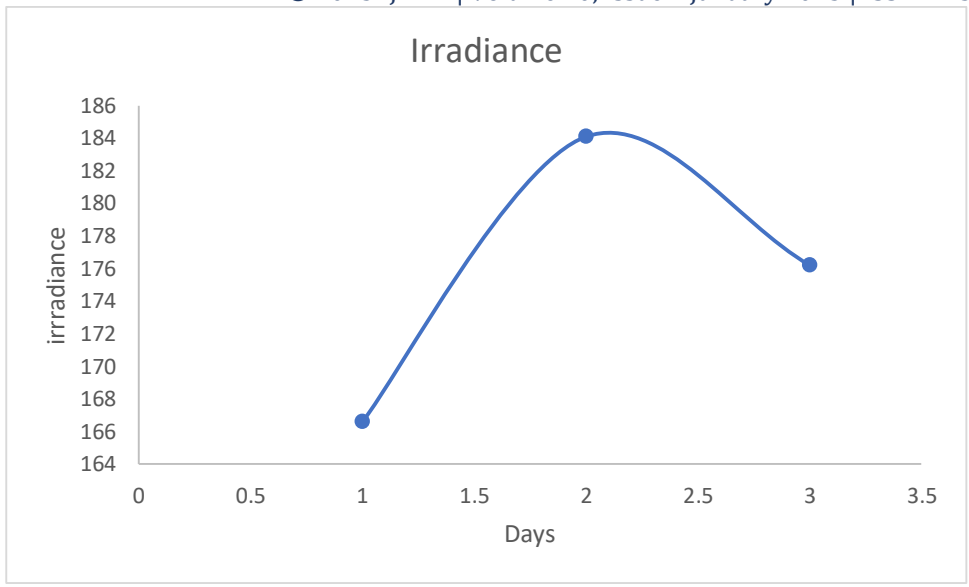


Fig. 24: comparing the average irradiance of days readings without heat collector

Fig 24 compares the average irradiance of the first three day of experimentation and shows that the highest irradiance was on the second day (184.1 W/m^2) and the lowest irradiance on the first day (166.6 W/m^2). The chat flow corresponds with the outlet temperature at fig. 23.

Table 4.8: Comparing the average temperature, irradiance and efficiency for the heater with heat collector.

Days	Ambient	Outlet	Irradiance	Efficiency
	Temperature	temperature	(W/m^2)	(%)
nten	(°C)	(°C)	earch	Jour
4	49.0	38.0	672.3	93.9
5	36.2	51.0	508.4	111.9
6	<mark>36.7</mark>	58.0	723.0	97.8

Table 4.8 has its efficiency exceeding 100% on day five which would have resulted to high record of thermal energy utilization from the collector during the cloud interruption hours as shown in table 4.5.

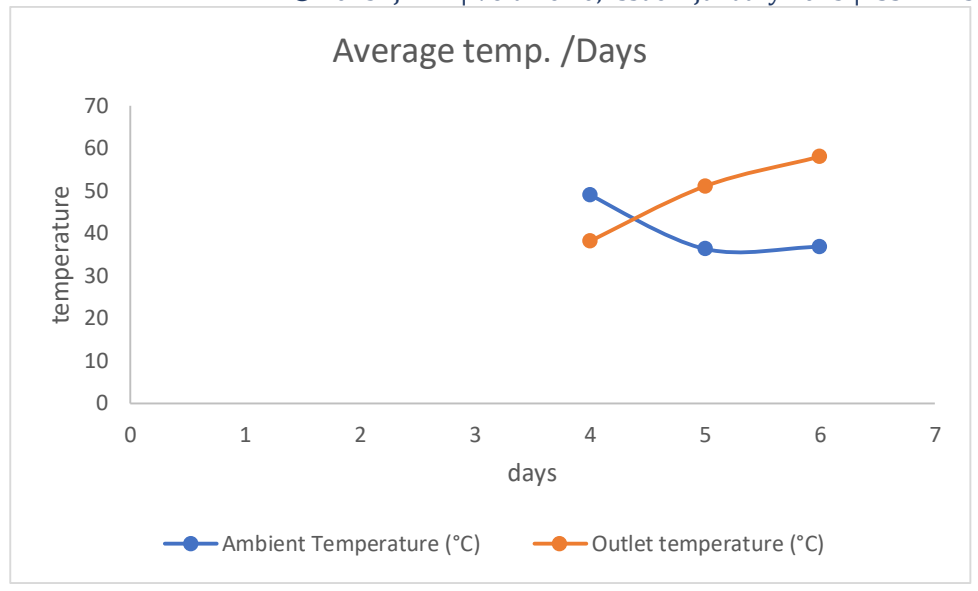


Fig. 25: comparing the average temperature of days readings with heat collectors

Fig. 25 shows an interwoven chart between the average ambient temperature and average outlet temperature. On the days the experiment was conducted ambient temperature was recorded at 49 °C against outlet temperature at 38 °C. On day six, the average outlet temperature was recorded to be 58 °C against the average ambient temperature at 38 °C.

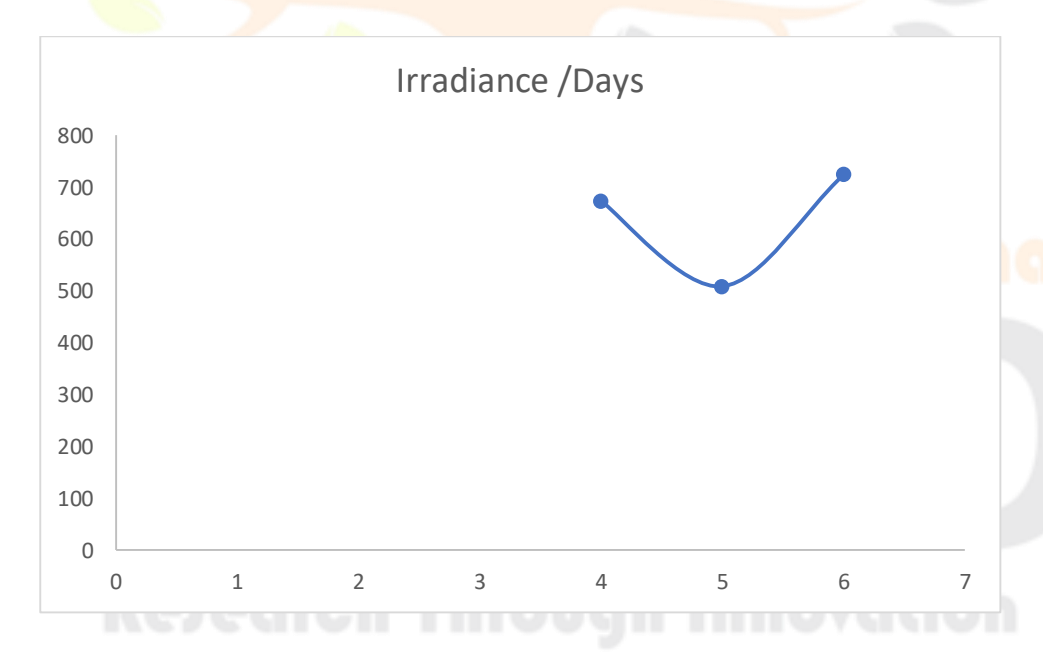


Fig. 26: comparing the average irradiance of days readings with heat collectors

Fig. 26 shows the highest irradiance on day six (723 W/ m^2) and the lowest at day five (508.4 W/ m^2).

Results and discussions

It is seen from the overall results that the irradiance levels and the output temperature are closely related. For the first three days of testing without the thermal energy collector, an outlet temperature of 37.1 °C was the highest temperature observed. However, for the last three days of testing using the thermal energy collector, the

maximum outlet temperature observed was 58 °C. This clearly shows that the system performs better using the thermal energy collector. The system was designed with a desired output temperature of 70 °C and the collector area used was $0.42m^2$ obtained during the design process. The designed temperature was attained at the outlet temperature (72.0 °C) as seen in table 4.4. The total volume of water heated up was 10-litres.

(Ekpo. J & Enyinma, 2017) designnature a solar water heater to provide 75 litres of water at 60 °C daily. From their design, the collector area required was $1.464 \ m^2$. However, they used an area of $2.3m^2$ during the construction of their system and obtained a maximum output of 76 °C. Comparing the two results shows that although (Ekpo. J & Enyinma, 2017) used a larger collector area, their peak outlet temperature was slightly higher than the peak value obtained in this work. This shows that using a larger collector area would not necessarily improve performance, the irradiance available at the system site also plays a role on system performance.

The highest irradiance level of 1074.0 W/m^2 was observed on day six, the highest outlet temperature of $72 \,^{\circ}\text{C}$ was also observed on the same day and at the same time. The highest rise in outlet temperature was observed on day four with a temperature rise of $47.1 \,^{\circ}\text{C}$ between ten am and noon. It is noteworthy that day three had the lowest irradiance levels. The highest efficiency gotten from the system was 98% on day four at 3:15pm. The highest thermal energy dissipation was recorded from 4:15pm to 5:45pm at day four.

5 CONCLUSION

The development of a 10-litre capacity Parabolic Trough Solar Water Heater concentrator was carried. The system was tested, and the following results were observed. From the first three days of testing which was done without a thermal collector, the highest outlet temperature recorded was 51.3 °C by 2:15pm at day two. For the last three days of testing with the thermal collector, the highest outlet temperature recorded was 72.0 °C at 12:45pm. This difference clearly shows that the system performs better during the dry season when the irradiance levels are higher. The highest irradiance recorded was 1074.0 W/ m^2 on the fourth day of testing while the highest efficiency recorded from the system was 98% at 3:15pm on day four.

REFERENCES

- Adedayo, H.B. (2021). Energy research in Nigeria: A bibliometric analysis. Elsevier, 1.
- Agbetuyi, S. O. Oyedepo, C. O. A. (2018). The Vast Renewable Energy in Africa versus its Slow. *International Electrical Engineering Journal*.
- Astolfi, M. (Eds.), et al. (2017). Organic Rankine Cycle (ORC) Power Systems. Elsevier.
- Aziz, J., et al. (2014). Concentrateurs solaires et production électrique, Institut National des Sciences Appliquées de Rouen (INSA). Département Sciences et Techniques pour L'ingénieur, 685 Avenue de L'université BP 08-76801 Saint-Etienne-Du-Rouvray.
- Bahman., Zohuri. (2017). Compact Heat Exchangers Application in New Generation of CSP. ResearchGate.
- Magal B.S., (1993). Solar Power Engineering. Tata McGraw Hill Publishing Company Limited, New Delhi.
- Barry, C. (2018). thermal properties of glass fiber thread. *B&W FIBERGLASS NEWS*, *1*. http://info.bwfiberglass.com/blog/the-thermal-properties-of-glass-fiber-thread.
- Dabija, A. (2020). Theory to Practice and All the Way Back. Designing with The Sun. In: Visa I., Duta A. (eds)

 Solar Energy Conversion in Communities. Springer Proceedings in Energy. Springer, Cham.

 https://doi.org/10.1007/978-3-030-55757-7_36.
- Djamel Benmenine, Mokhtar Ghodbane, Abderrahmane Khechekhouche, Boussad Boumeddane. (november 2020). Brief on Solar Concentrators: Differences and Applications. *reseachgate.net*.
- Egyptophile, L. (accessed on Jan. 31, 2022). une histoire d'énergie solaire. https://egyptophile.blogspot.com/2015/04/legypte-une-histoire-denergie-solaire.html,.
- Ekechukwu O. V. (2011). Domestic Hot Water Requirement Profile In Nigeria. researchGate.
- Exergia. (2009). European Commission Directorate General Energy and Transport . *Evaluation, April.*http://exergia.gr/wp-content/uploads/materials-domestic-water.pdf.
- Fernandez-Garcia, A., E. Zarza, L. Valenzuela, M. Perez. (2010). Parabolic-trough solar collectors and their applications. *Renewable and Sustainable Energy Reviews*, 1695-1721.

- Gadalla. Mahmoud, (2018). A concise overview of heliostat fields-solar thermal collectors: Current state of art and future perspective. wiley energy research.
- Garg, H. P. & Prakash, J. (2000). Solar Energy. Tata McGraw-Hill, New delhi.
- Ghodbane, M.(2016). A linear Fresnel reflector as a solar system for heating water: Theoretical and experimental study. *Case Studies in Thermal Engineering*, 8 (c), 176-186.
- Ghodbane, M.,. (2017). A parabolic trough solar collector as a solar system for heating water: a study based on numerical simulation. *International Journal of Energetica (IJECA)*, 29-37.
- Ghodbane, M. (2016). Study and numerical simulation of solar system for air heating. *ournal of Fundamental* and Applied Sciences, 40-60.
- Gong, J., & Sumathy, K. (2016). Active solar water heating systems. In Advances in Solar Heating and Cooling.

 Elsevier Ltd.
- Grange, B. (2014). simulation of a hybrid solar gas-turbine cycle with storage integration. *Energy Procedia*, 49: 1147-1156. https://doi.org/10.1016/j.egypro.2014.03.124.
- Hukman., H. (2004). Progress of Solar power plant. Sol Energy (in Chinese), 3:43-4.
- Hess, S. (n.d.). Solar thermal process heat (SPH). Stellenbosch University, Stellenbosch, South Africa.
- Jui. Sheng., Hseih. (1986). Solar Energy Engineering. Prentice-Hall, Inc., Englewood Cliffs, New Jersey.
- Kalogirou, S. (2003). The potential of solar industrial process heat applications. Appl. Energy 76, 337–361.
- Kalogirou, S. (2009). Solar Energy Engineering: Processes and Systems. 1st ed., Academic Press 2009.
- Key world energy statistics. (2015). *International Energy Agency (IEA)*.
- Komen, J. (2 May 2015, 09:36). A solar power system built in 1983 that used mirrors to heat up molten salts coolant to 450 °C. http---en.wikipedia.org-wiki-Themis (solar power plant) (20251694405).jpg.
- Larrouturou, F.; Caliot, C.; Flamant, G. (2016). Influence of receiver surface spectral selectivity on the solar-toelectric efficiency of a solar tower power plant. *solar energy*.

- Leutz, R. (2001). Nonimaging Fresnel Lenses, Springer Series in Optical Sciences. *Springer Berlin Heidelberg*, *Berlin, Heidelberg*.
- Library, S. (2020). Lavoisier's solar furnace. https://www.sciencephoto.com/media/363956/view/lavoisier-s-solar-furnace.
- Lovegrove K. (2012). Fundamental principles of concentrating solar power (CSP) systems. *Woodhead publishing*, chapter 2.
- Nwoke O.(2015). Country Market Report on Solar Thermal Heating Systems Nigeria.
- perlin, J. (2008). Workhorse of the Solar Industry Pacific Standard. https://psmag.com/environment/workhorse-of-the-solar-industry-4736.
- Pytilinski, J. (1978). Solar energy installations for pumping irrigation water. Solar Energy, 21(4), 255-262.
- Rogers G. F. (1981). Thermodynamic and Transport Properties of Fluids. 3rd edn, Oxford.
- Said, Z. (2020). Heat transfer, entropy generation, economic and environmental analyses of linear fresnel reflector using novel rGO-Co3O4 hybrid nanofluids. *Renewable Energy*, 165 (part 1), 420-437.
- Sarbu, I. (2016). Solar Heating and Cooling Systems. *Elsevier Inc.*
- Sharma S. (2015). Solar Cells: In Research and Applications—A Review. *Materials Sciences and Applications*.
- Silvi, C. (1980). ISES-ITALIA Section of the International Solar Energy Society. 1980). ISES-Italia (1964-1980), 235-258.
- Silvi, C. (2009). The pioneering work on linear Fresnel reflector concentrators (LFCs) in Italy. S. Paces (Ed.)

 15th Solar Paces Conference, Solar Power and Chemical Energy Systems, Berlin, Germany.
- Solar thermal electricity. (2014). *International Energy Agency (IEA)*. *Technology roadmap*.
- Soulen, R. (1996). James Dewar, his flask and other achievements. *Physics Today*, 49(3), 32-37.
- Stine W. B. (1985). Solar Energy Fundamentals and Design. John Wiley and Sons Inc., New York.
- Thombare, D. (2008). Technological development in the Stirling cycle engine. *Renewable and Sustainable Energy Reviews*,.

ToolBox, E. (2005). Water Flow in Copper Tubes - Pressure Loss due to Fricton https://www.engineeringtoolbox.com/pressure-loss-copper-pipes-d_930.html.

Uwah., E. J. (2020). Design and construction of a portable solar water heater. abuja: wikipedia.

Zheng, H. (2017). Solar concentrating directly to drive desalination technologies, in: Solar Energy Desalination Technology. *Elsevier*,.

